


 Cite this: *Chem. Commun.*, 2021, 57, 7910

 Received 4th June 2021,  
Accepted 6th July 2021

DOI: 10.1039/d1cc02956h

rsc.li/chemcomm

## SARS-CoV-2 M<sup>Pro</sup> inhibition by a zinc ion: structural features and hints for drug design†

 Deborah Grifagni,<sup>id a</sup> Vito Calderone,<sup>id abc</sup> Stefano Giuntini,<sup>a</sup>  
Francesca Cantini,<sup>id \*abc</sup> Marco Fragai,<sup>id \*abc</sup> and Lucia Banci<sup>id \*abc</sup>

**Structural data on the SARS-CoV-2 main protease in complex with a zinc-containing organic inhibitor are already present in the literature and gave hints on the presence of a zinc binding site involving the catalytically relevant cysteine and histidine residues. In this paper, the structural basis of ionic zinc binding to the SARS-CoV-2 main protease has been elucidated by X-ray crystallography. The zinc binding affinity and its ability to inhibit the SARS-CoV-2 main protease have been investigated. These findings provide solid ground for the design of potent and selective metal-conjugated inhibitors of the SARS-CoV-2 main protease.**

The SARS-CoV-2 main protease (SARS-CoV-2 M<sup>Pro</sup>), also referred to as 3-chymotrypsin-like protease (SARS-CoV-2 3CL<sup>Pro</sup>) or nsp5 is a cysteine protease that hydrolyses viral polyproteins at several sites with a preference for the Leu-Gln (Ser, Ala, Gly) sequences.<sup>1</sup> The protein exhibits 96% sequence identity and a very high structural similarity with the SARS-CoV M<sup>Pro</sup> protein.<sup>2,3</sup> The enzyme represents one of the main drug-target candidates for covid-19 infection because it features a large and deep pocket at the active site and is crucial for viral replication.<sup>3-5</sup> Presently more than 280 crystal structures of SARS-CoV-2 M<sup>Pro</sup> with covalently or non-covalently bound inhibitors or chemical fragments have been deposited into the protein data bank (PDB, <https://www.rcsb.org/>). The active form of the enzyme is a homodimer (67.6 kDa) where the N-terminal region of each monomer interacts with the Glu166 of the other,

thus promoting and stabilizing binding of the substrate.<sup>3,4</sup> The active sites in each monomer face away from one another and are formed by a Cys-His dyad (Cys 145 and His 41). The hydrolysis of the substrate takes place in two main steps named acylation and deacylation. During the first step, an acyl-enzyme complex is formed, *via* a covalent bond with the S<sub>γ</sub> atom of Cys 145, with the release of a fragment of the substrate. During deacylation, the acyl-enzyme complex is released by the action of a water molecule, thus recovering the protease to its active state for a new catalytic cycle.<sup>6,7</sup> Several inhibitors of SARS-CoV and SARS-CoV-2 M<sup>Pro</sup> have been designed that interfere with the formation of the acyl-enzyme complex due to the promotion of a covalent bond between the thiol group of the catalytic cysteine and the inhibitor.<sup>3,4,8</sup>

A similar approach has been exploited using zinc-coordinating inhibitors,<sup>9,10</sup> where the zinc ion plays a role in stabilizing the protein-inhibitor complex through a tetrahedral coordination shared by the active site cysteine and histidine with two donor atoms of the inhibitor. The solved experimental structures<sup>9-11</sup> however leave open interesting questions concerning the zinc binding ability of the protease in the cellular environment, even in the absence of a coordinating ligand, and the possible role of zinc ions in modulating its biological activity. Moreover, a recently published bioinformatics study<sup>12</sup> stimulated our interest on the possible role of zinc in covid-19 infection and therapy.<sup>13</sup>

Zinc is second to iron as the most abundant transition metal ion in living organisms.<sup>14</sup> In eukaryotes, 9–10% of proteins are zinc-binding proteins that depend on this metal ion to carry out their biological function. Zinc is involved in proliferation, cell signaling, differentiation, oxidative stress and immune response and many other cellular processes.<sup>15,16</sup> It is well known that extracellular and intracellular zinc levels are tightly regulated in such a way that free zinc ions (Zn<sup>2+</sup>) represent a minimal fraction of total cellular zinc (~0.0001%).<sup>17-20</sup> Furthermore, zinc ions are not homogeneously distributed within the cells, with large differences among cellular compartments and organelles.<sup>21,22</sup>

Zinc has a key role in the signalling pathways of the innate and adaptive immune reactions.<sup>23,24</sup> It has been reported that

<sup>a</sup> Magnetic Resonance Center (CERM), University of Florence, via Sacconi 6, Sesto Fiorentino, 50019, Italy. E-mail: francesca.cantini@unifi.it, marco.fragai@unifi.it, lucia.banci@unifi.it

<sup>b</sup> Department of Chemistry "Ugo Schiff", University of Florence, via della Lastruccia 3, Sesto Fiorentino, 50019, Italy

<sup>c</sup> Consorzio Interuniversitario Risonanze Magnetiche MetalloProteine (CIRMMMP), via Sacconi 6, Sesto Fiorentino, 50019, Italy

† Electronic supplementary information (ESI) available: SARS-CoV-2 M<sup>Pro</sup> expression and purification, crystallographic data, NMR spectroscopy and enzymatic activity data. Apo and zinc bound SARS-CoV-2 M<sup>Pro</sup> structures have been deposited at the PDB (PDB ID codes: 7NXH and 7NWX, respectively). See DOI: 10.1039/d1cc02956h



zinc is able to participate in many processes of defense against infections.<sup>25</sup> Experimental and clinical evidence exists that assesses zinc as a direct antiviral, as well as a stimulant of antiviral immunity. For example, *in vitro* replication of the influenza virus is significantly decreased by the addition of the zinc ionophore pyrrolidine dithiocarbamate.<sup>26</sup> Likewise, severe acute respiratory syndrome (SARS) coronavirus RdRp template binding and elongation was inhibited by zinc in Vero-E6 cells.<sup>27</sup> Furthermore, zinc salts were shown to inhibit respiratory syncytial virus.<sup>28</sup> Therefore, the supplementation of zinc has been proposed to treat viral infections. In particular, the role of zinc as an antiviral could be dual: on one side, zinc supplementation could improve the antiviral response and systemic immunity in patients with zinc deficiency,<sup>29</sup> and, on the other side, zinc treatment could inhibit viral replication or infection-related symptoms.<sup>30</sup>

In this respect, advances in understanding the role of zinc in covid-19 pathogenesis require the characterization of the viral zincosome, and particularly how the different SARS-CoV-2 proteins interact with this metal ion.

Here, we provide an important piece of the puzzle by reporting the X-ray structure of SARS-CoV-2 M<sup>Pro</sup> both in the apo form and in complex with an isolated zinc ion, and an extensive biophysical analysis of the metal–protein interaction properties in solution.

Crystals of apo SARS-CoV-2 M<sup>Pro</sup> were soaked for two days with 1.5 mM of the zinc ion solution (see the ESI† and Fig. S1 for experimental details). The apo protein structure discussed in this paper is totally superimposable with the others already deposited in the PDB along the entire sequence. The structure of Zn-bound SARS-CoV-2 M<sup>Pro</sup> (ESI,† Fig. S2) resembles that of the apo protein with average backbone and heavy atom RMSD values of 0.19 Å and 0.64 Å, respectively. Only the local loop regions showed backbone RMSD values higher than average (ESI,† Fig. S3). The electron density for the zinc ion is very well defined and the metal is present at full occupancy (Fig. 1a).

The zinc ion is coordinated by the sulfur atom of Cys145, the N $\epsilon$  atom of the imidazole ring of His41, a well-defined water molecule and a more labile one shuttling between two positions, thus completing a tetrahedral geometry. This is the first structure with a zinc ion bound to coronavirus M<sup>Pro</sup> (or homologous proteins in other viruses) as a cation, rather than as part of a coordination compound. Comparison of the present structure with that of apo SARS-CoV-2 M<sup>Pro</sup> shows that the residues involved in zinc binding do not undergo a significant structural rearrangement, supporting the idea that the binding site is ready to accommodate the metal (Fig. 1b and ESI,† Fig. S4).

The interaction of SARS-CoV-2 M<sup>Pro</sup> with the zinc ion has been also investigated in solution using NMR. <sup>15</sup>N isotopically enriched protein samples (at a concentration of 130  $\mu$ M as the monomer) were titrated with the zinc ion and monitored using 1D <sup>1</sup>H and 2D <sup>1</sup>H–<sup>15</sup>N TROSY HSQC NMR spectroscopy (Fig. 2). Spectral changes were observed that indicate an intermediate-to-slow regime on the NMR time scale between the free and bound forms. Fig. 2b shows the methyl signal for both the apo- and metal-bound forms in a slow exchange regime.

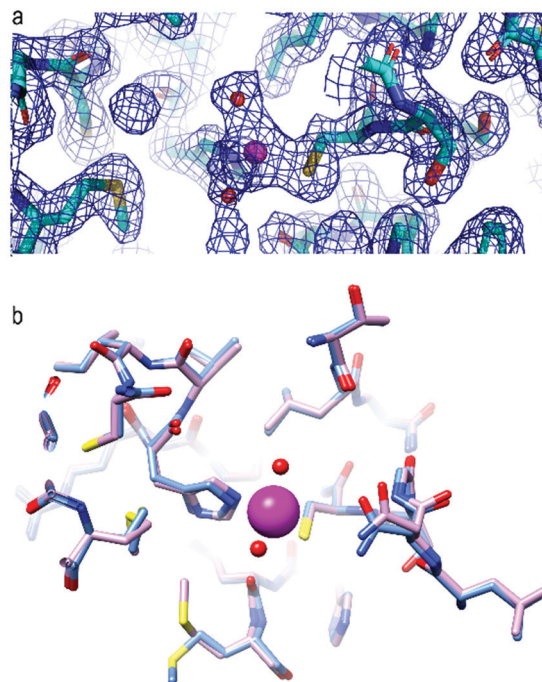


Fig. 1 (a)  $2F_o - F_c$  electron density map contoured at the  $1\sigma$  level showing the zinc binding site in zinc bound SARS-CoV-2 M<sup>Pro</sup>. The zinc ion is shown as a magenta sphere, the water molecules are shown as red spheres. (b) Superposition of zinc bound SARS-CoV-2 M<sup>Pro</sup> (light blue) and SARS-CoV-2 apo M<sup>Pro</sup> (pink) showing zinc (magenta) coordinated by Cys145 and His41 and two water molecules (red) completing the zinc coordination environment.

This observation indicates that the zinc ion binds SARS-CoV-2 M<sup>Pro</sup> in solution.

To estimate the affinity of the zinc ion for the protein and to investigate its effect on the proteolytic activity of the enzyme, a fluorimetric assay was carried out by monitoring the fluorescence increase due to the hydrolysis of the peptide substrate (Mca-AVLQ ↓ SGFR-K(Dnp)K).<sup>4</sup> The addition of zinc ions inhibits the proteolytic activity of the enzyme, which is consistent with the interaction of zinc with the protein active site in solution. The fit of the kinetic data provided a  $K_i$  value of  $0.58 \pm 0.19 \mu$ M (see ESI,† Fig. S5 and Fig. 3).

The binding capability of SARS-CoV-2 M<sup>Pro</sup> towards the zinc ion is not completely unexpected as homologous proteases are reported to bind a zinc ion, not in its ionic form but as a metal-conjugated ligand. A comparison of the present structure with those of homologous proteases expressed by other viruses closely related to SARS-CoV-2 such as SARS-CoV (2Z9J, 2Z9K, 2Z9L, 2Z9G and 2Z94), Coxsackievirus B3 (2ZTX), HCoV-229E (2ZU2) and with the only report in the literature of a SARS-CoV-2 M<sup>Pro</sup> structure bound with zinc pyridone (7B83) showed that, overall, the zinc binding site is well maintained with non-significant deviations from one structure to another (Fig. 4).

The zinc binding site has been also compared with that of other non-viral cysteine-proteases reported to bind zinc, such as cathepsin S both in the metal-bound and metal-free state (2HH5 and 2HHN), or enzymes such as dimethylarginine dimethylaminohydrolase I (2CI7). The structural features of



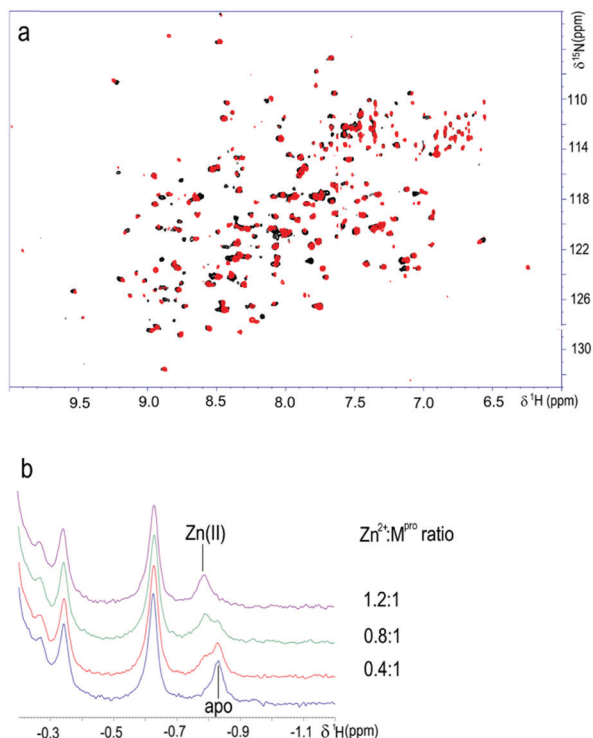


Fig. 2 (a) Superposition of 2D  $^1\text{H}$ - $^{15}\text{N}$  TROSY HSQC spectra of apo SARS-CoV-2  $\text{M}^{\text{Pro}}$  (black) and zinc-bound  $\text{M}^{\text{Pro}}$  at a 1.2:1  $\text{Zn}^{2+}:\text{M}^{\text{Pro}}$  ratio (red); (b) detail of the methyl region of the 1D  $^1\text{H}$  NMR spectra showing  $\text{M}^{\text{Pro}}$  titration with  $\text{Zn}^{2+}$ .

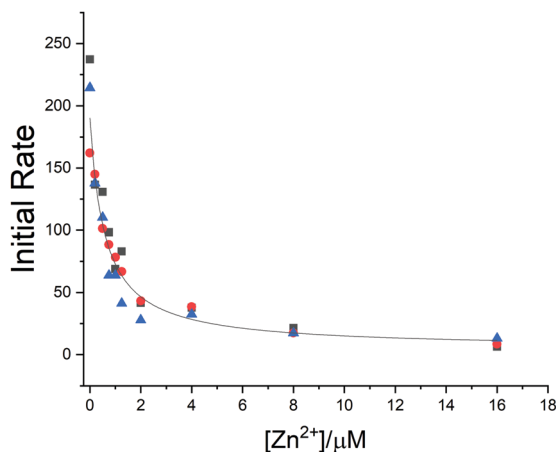


Fig. 3 Zinc inhibits the activity of SARS-CoV-2  $\text{M}^{\text{Pro}}$ . The hydrolytic activity of SARS-CoV-2  $\text{M}^{\text{Pro}}$  was measured in the presence of increasing concentrations of the zinc ion. Three independent measurements are shown as red circles, blue triangles and black squares, respectively. The  $K_i$  values were determined using nonlinear regression.

the zinc binding site in these systems are very similar to those of SARS-CoV-2  $\text{M}^{\text{Pro}}$ .

The structural analysis and the inhibition activity of zinc towards SARS-CoV-2  $\text{M}^{\text{Pro}}$  suggest interesting considerations on how the metal ion and the viral protease could interplay in the cells. The affinity of the protein for zinc, although high, appears

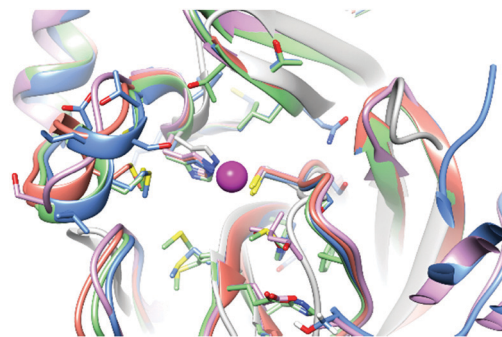


Fig. 4 Superposition of the zinc binding site in zinc bound SARS-CoV-2  $\text{M}^{\text{Pro}}$  (light blue), 2Z94 (red), 2ZU2 (pink), 7B83 (green) and 2ZTX (gray).

to be not sufficient to inactivate SARS-CoV-2  $\text{M}^{\text{Pro}}$  as almost all the intracellular zinc ion is bound to other proteins with similar or higher affinity. This is confirmed by the efficient viral replication and spreading of covid-19 infection and by the observation that proteins bearing the same metal binding site such as cathepsin S are highly active inside cells. For the same reasons, the potential use of zinc supplementation for SARS-CoV-2  $\text{M}^{\text{Pro}}$  inhibition does not seem viable. In particular, the presence of many zinc-binding proteins with similar or higher affinity would make a selective inhibition of SARS-CoV-2  $\text{M}^{\text{Pro}}$  by zinc supplementation unlikely. More promising for SARS-CoV-2  $\text{M}^{\text{Pro}}$  inhibition would be the design of suitable metallodrugs that incorporate zinc. A zinc-containing organic or peptidomimetic molecule, by simultaneously interacting with the catalytically relevant Cys-His dyad and with neighbouring additional sites or allosteric sites,<sup>11</sup> could be the basis for the design of inhibitors with low nanomolar affinity for SARS-CoV-2  $\text{M}^{\text{Pro}}$ .<sup>31,32</sup> This is not the case for zinc-pyrithione where the organic fragments stick-out from the protein surface without establishing any significant interaction with the protein (Fig. S6, ESI<sup>†</sup>). In contrast, the combination of the inhibitory effect of zinc with that of a molecule interacting with residues surrounding the catalytic dyad can be a strategy for the design of promising inhibitors. A similar approach has been exploited to develop inhibitors of zinc-dependent matrix metalloproteinases.<sup>33,34</sup> In addition, our results suggest that drugs based on alternative metal ions, such as platinum or gold, could be investigated as potential SARS-CoV-2  $\text{M}^{\text{Pro}}$  inhibitors considering they are well established binders of cysteine thiolates.<sup>35,36</sup>

In summary, the present study highlights that a zinc ion inhibits SARS-CoV-2  $\text{M}^{\text{Pro}}$  by binding at the active site in a similar way to that observed for other cysteine proteases. The affinity of the protein for the metal ion has been experimentally determined and it does not seem high enough for any real therapeutic application of zinc supplementation, at least in its ionic state. However, our results suggest that a zinc ion coordinated to suitable ligands capable of interacting with additional sites on the protein surface could provide a significant increase in binding affinity, thus allowing the design of potent and more selective inhibitors of SARS-CoV-2  $\text{M}^{\text{Pro}}$ .

Instruct-ERIC, a landmark ESFRI project, and specifically the CERM/CIRMMIP Italy centre are acknowledged. Moreover, the authors acknowledge H2020 – INFRAIA iNEXT-Discovery – Structural



Biology Research Infrastructures for Translational Research and Discovery (contract no. 871037) and Fondazione Cassa di Risparmio di Firenze, project title “Dalla Struttura tridimensionale di antigeni proteici all’ottimizzazione di potenziali candidati vaccini”.

## Conflicts of interest

There are no conflicts to declare.

## Notes and references

- 1 W. Rut, K. Groborz, L. Zhang, X. Sun, M. Zmudzinski, B. Pawlik, X. Wang, D. Jochmans, J. Neyts, W. Mlynarski, R. Hilgenfeld and M. Drag, *Nat. Chem. Biol.*, 2021, **17**, 222–228.
- 2 K. Anand, J. Ziebuhr, P. Wadhvani, J. R. Mesters and R. Hilgenfeld, *Science*, 2003, **300**, 1763–1767.
- 3 L. Zhang, D. Lin, X. Sun, U. Curth, C. Drosten, L. Sauerhering, S. Becker, K. Rox and R. Hilgenfeld, *Science*, 2020, **368**, 409–412.
- 4 Z. Jin, X. Du, Y. Xu, Y. Deng, M. Liu, Y. Zhao, B. Zhang, X. Li, L. Zhang, C. Peng, Y. Duan, J. Yu, L. Wang, K. Yang, F. Liu, R. Jiang, X. Yang, T. You, X. Liu, X. Yang, F. Bai, H. Liu, X. Liu, L. W. Guddat, W. Xu, G. Xiao, C. Qin, Z. Shi, H. Jiang, Z. Rao and H. Yang, *Nature*, 2020, **582**, 289–293.
- 5 A. Douangamath, D. Fearon, P. Gehrtz, T. Krojer, P. Lukacik, C. D. Owen, E. Resnick, C. Strain-Damerell, A. Aimon, P. Abranyi-Balogh, J. Brandao-Neto, A. Carbery, G. Davison, A. Dias, T. D. Downes, L. Dunnett, M. Fairhead, J. D. Firth, S. P. Jones, A. Keeley, G. M. Keseru, H. F. Klein, M. P. Martin, M. E. M. Noble, P. O'Brien, A. Powell, R. N. Reddi, R. Skynner, M. Snee, M. J. Waring, C. Wild, N. London, F. von Delft and M. A. Walsh, *Nat. Commun.*, 2020, **11**, 5047.
- 6 J. Lee, L. J. Worrall, M. Vuckovic, F. I. Rosell, F. Gentile, A. T. Ton, N. A. Caveney, F. Ban, A. Cherkasov, M. Paetzel and N. C. J. Strynadka, *Nat. Commun.*, 2020, **11**, 5877.
- 7 J. Solowiej, J. A. Thomson, K. Ryan, C. Luo, M. He, J. Lou and B. W. Murray, *Biochemistry*, 2008, **47**, 2617–2630.
- 8 C. A. Ramos-Guzman, J. J. Ruiz-Pernia and I. Tunon, *ACS Catal.*, 2021, **11**, 4157–4168.
- 9 C. C. Lee, C. J. Kuo, M. F. Hsu, P. H. Liang, J. M. Fang, J. J. Shie and A. H. Wang, *FEBS Lett.*, 2007, **581**, 5454–5458.
- 10 C. C. Lee, C. J. Kuo, T. P. Ko, M. F. Hsu, Y. C. Tsui, S. C. Chang, S. Yang, S. J. Chen, H. C. Chen, M. C. Hsu, S. R. Shih, P. H. Liang and A. H. Wang, *J. Biol. Chem.*, 2009, **284**, 7646–7655.
- 11 S. Günther, P. Y. A. Reinke, Y. Fernández-García, J. Lieske, T. J. Lane, H. M. Ginn, F. H. M. Koua, C. Ehrh, W. Ewert, D. Oberthuer, O. Yefanov, S. Meier, K. Lorenzen, B. Krichel, J. D. Kopicki, L. Gelisio, W. Brehm, I. Dunkel, B. Seychell, H. Gieseler, B. Norton-Baker, B. Escudero-Pérez, M. Domaracky, S. Saouane, A. Tolstikova, T. A. White, A. Hänle, M. Groessler, H. Fleckenstein, F. Trost, M. Galchenkova, Y. Gevorkov, C. Li, S. Awel, A. Peck, M. Barthelmeß, F. Schlünzen, P. Lourdu Xavier, N. Werner, H. Andaleeb, N. Ullah, S. Falke, V. Srinivasan, B. A. França, M. Schwinzer, H. Brognaro, C. Rogers, D. Melo, J. J. Zaitseva-Doyle, J. Knoska, G. E. Peña-Murillo, A. R. Mashhour, V. Hennicke, P. Fischer, J. Hakanpää, J. Meyer, P. Gribbon, B. Ellinger, M. Kuzikov, M. Wolf, A. R. Beccari, G. Bourenkov, D. von Stetten, G. Pompidor, I. Bento, S. Panneerselvam, I. Karpics, T. R. Schneider, M. M. Garcia-Alai, S. Niebling, C. Günther, C. Schmidt, R. Schubert, H. Han, J. Boger, D. C. F. Monteiro, L. Zhang, X. Sun, J. Pletzer-Zelgert, J. Wollenhaupt, C. G. Feiler, M. S. Weiss, E. C. Schulz, P. Mehrabi, K. Karničar, A. Usenik, J. Loboda, H. Tidow, A. Chari, R. Hilgenfeld, C. Uetrecht, R. Cox, A. Zaliani, T. Beck, M. Rarey, S. Günther, D. Turk, W. Hinrichs, H. N. Chapman, A. R. Pearson, C. Betzel and A. Meents, *Science*, 2021, **372**, 642–646.
- 12 A. Pormohammad, N. K. Monych and R. J. Turner, *Int. J. Mol. Med.*, 2021, **47**, 326–334.
- 13 I. Wessels, B. Rolles and L. Rink, *Front. Immunol.*, 2020, **11**, 1712.
- 14 C. Andreini, L. Banci, I. Bertini and A. Rosato, *J. Proteome Res.*, 2006, **5**, 3173–3178.
- 15 D. Beyersmann and H. Haase, *Biometals*, 2001, **14**, 331–341.
- 16 D. D. Marreiro, K. J. Cruz, J. B. Morais, J. B. Beserra, J. S. Severo and A. R. de Oliveira, *Antioxidants*, 2017, **6**.
- 17 R. A. Bozym, R. B. Thompson, A. K. Stoddard and C. A. Fierke, *ACS Chem. Biol.*, 2006, **1**, 103–111.
- 18 M. Malavolta, L. Costarelli, R. Giacconi, E. Muti, G. Bernardini, S. Tesei, C. Cipriano and E. Mocchegiani, *Cytometry A*, 2006, **69**, 1043–1053.
- 19 J. L. Vinkenborg, T. J. Nicolson, E. A. Bellomo, M. S. Koay, G. A. Rutter and M. Merckx, *Nat. Methods*, 2009, **6**, 737–740.
- 20 D. J. Eide, *Biochim. Biophys. Acta*, 2006, **1763**, 711–722.
- 21 D. Osman, M. A. Martini, A. W. Foster, J. Chen, A. J. P. Scott, R. J. Morton, J. W. Steed, E. Lurie-Luke, T. G. Huggins, A. D. Lawrence, E. Deery, M. J. Warren, P. T. Chivers and N. J. Robinson, *Nat. Chem. Biol.*, 2019, **15**, 241–249.
- 22 T. R. Young, M. A. Martini, A. W. Foster, A. Glasfeld, D. Osman, R. J. Morton, E. Deery, M. J. Warren and N. J. Robinson, *Nat. Commun.*, 2021, **12**, 1195.
- 23 M. Maywald, I. Wessels and L. Rink, *Int. J. Mol. Sci.*, 2017, **18**.
- 24 J. R. de Jesus and T. de Araújo Andrade, *Metallomics*, 2020, **12**, 1912–1930.
- 25 S. R. Hennigar and J. P. McClung, *Am. J. Lifestyle Med.*, 2016, **10**, 170–173.
- 26 U. Noboru, O. Kunio, B. Toshio, Y. Bo and Y. Toshio, *Antiviral Res.*, 2002, **56**, 207–217.
- 27 A. J. W. te Velthuis, S. H. E. van den Worm, A. C. Sims, R. S. Baric, E. J. Snijder and M. J. van Hemert, *PLoS Pathog.*, 2010, **6**, e1001176.
- 28 R. O. Suara and J. E. Crowe, *Antimicrob. Agents Chemother.*, 2004, **48**, 783–790.
- 29 A. S. Prasad, *J. Am. Coll. Nutr.*, 2009, **28**, 257–265.
- 30 S. A. Read, S. Obeid, C. Ahlenstiel and G. Ahlenstiel, *Adv. Nutr.*, 2019, **10**, 696–710.
- 31 S. Johnson, E. Barile, B. Farina, A. Purves, J. Wei, L.-H. Chen, S. Shiryayev, Z. Zhang, I. Rodionova, A. Agrawal, S. M. Cohen, A. Osterman, A. Strongin and M. Pellicchia, *Chem. Biol. Drug Des.*, 2011, **78**, 211–223.
- 32 A. Agrawal, S. L. Johnson, J. A. Jacobsen, M. T. Miller, L.-H. Chen, M. Pellicchia and S. M. Cohen, *ChemMedChem*, 2010, **5**, 195–199.
- 33 I. Bertini, V. Calderone, M. Cosenza, M. Fragai, Y. M. Lee, C. Luchinat, S. Mangani, B. Terni and P. Turano, *Proc. Natl. Acad. Sci. U. S. A.*, 2005, **102**, 5334–5339.
- 34 L. A. Alcaraz, L. Banci, I. Bertini, F. Cantini, A. Donaire and L. Gonnelli, *J. Biol. Inorg. Chem.*, 2007, **12**, 1197–1206.
- 35 L. Banci, I. Bertini, O. Blazevits, V. Calderone, F. Cantini, J. Mao, A. Trapananti, M. Vieru, I. Amori, M. Cozzolino and M. T. Carri, *J. Am. Chem. Soc.*, 2012, **134**, 7009–7014.
- 36 C. Zoppi, L. Messori and A. Pratesi, *Dalton Trans.*, 2020, **49**, 5906–5913.

